Exotic Stars as Challenges to Evolution
ASP Conference Series, Vol. 279, 2002
C. A. Tout and W. Van Hamme, eds.

Imaging Ejecta from the Final Flash Star V605 Aql

Kenneth Hinkle, Richard Joyce, Steven Ridgway

NOAO, P.O. Box 26732, Tucson, Arizona 85726, USA

Laird Close

Steward Observatory, University of Arizona, 933 N. Cherry Avenue, Tucson, Arizona 85721, USA

Thomas Lebzelter, Josef Hron, Karin Andre

Institute for Astronomy, Türkenschanzstrasse 17, A1180 Vienna, Austria

Abstract. The cloud of ejecta resulting from a final helium shell flash in V605 Aql has been imaged in both optical emission lines and infrared continuum. The obscuring circumstellar dust cloud, whose effects were first seen in 1923, is shown to be bipolar, suggesting dust formation takes place in a disk surrounding this star. The ongoing stellar mass loss in V605 Aql is part of the final flash episode, which has been ongoing since 1919. The pre-final flash planetary nebula, A58, is nearly circular. This implies that significant changes in the mass loss process occur between the AGB and final flash stages.

1. The Final Flash of V605 Aql

White dwarfs can undergo a final helium shell flash during which they temporarily regain AGB luminosity. The prototype object is V4334 Sgr (Sakurai's star). The central star of an old planetary nebula, Sakurai's star began its final flash episode in late 1995. Spectra in 1996 revealed an early F supergiant pseudo-photosphere. This cooled in three years to a dust enshrouded object of color temperature $\sim$ 600 K. The luminosity remained constant, indicating that helium shell burning is continuing.

We now know that the same series of events took place in V605 Aql in the 1920's. V605 Aql is the central star of the old planetary nebula (PNe) A58. V605 Aql brightened and faded in 1919–1923. Now V605 Aql is faint, $V \sim 22$, and red, $K \sim 14.6$. As with Sakurai's star hydrogen on the stellar surface was consumed. Spectroscopy of the A58 PNe and V605 Aql central knot show that the PNe has a normal He/H ratio of $\sim$ 0.15, while in the central knot He/H $\sim$ 1.2, showing that 75% of the hydrogen was converted to helium (Guerrero & Manchado 1996).

V605 Aql was incorrectly classified as a slow nova when it underwent its helium shell flash in the 1920's. When V605 Aql became visually faint in the

late 1920's it was no longer observed and was largely forgotten until the 1980's. Clayton & DeMarco (1997) present a review of observations of this star, establishing the status of V605 Aql among the very small sample of stars observed undergoing a final helium shell flash.

More than 80 years have now passed since V605 Aql underwent its final flash episode. The cloud of ejecta from this event is now large enough to image. In this brief report we present some results from our imaging experiments with HST, Gemini North, and the 3.6-m ESO telescope. A more complete report can be found in Hinkle et al. (2003).

2. Images

HST imaging of V605 Aql was done using the WFPC2 camera. Based on previous optical spectroscopy (Guerrero & Manchado 1996), we selected two filters to isolate the [O III] 5007 Å and [N II] 6584 Å lines. The HST/WFPC field was large enough to include in the image the surrounding planetary nebula A58 which had originated from the previous (pre-final flash) AGB and white dwarf phase of V605 Aql. The images are shown in Fig. 1. Note that A58, while nearly circular, has a major axis aligned with the symmetry of the V605 Aql image.

Infrared imagery was obtained using the 8-m Gemini North telescope and the Hokupa'a adaptive optics system (Graves et al. 2000). These images in the J, H, and K' bands (1.2, 1.6, and 2.3 μm), show V605 Aql in the infrared continuum. V605 Aql was too faint to allow HST imaging in the visual continuum in the limited time allocated to our project. The continuum flux, which is the result of re-radiation of light from the central star by the grains, drops rapidly into the visual (Fig. 2).

The mid-infrared imager TIMMI2 on the 3.8-m telescope at ESO was used to image V605 Aql at 11.9 μm. The image was an unresolved point source at the diffraction limit of the telescope. This image was used to measure the 11.9 μm magnitude of the point source. Previous mid-IR measurements have used much larger apertures. This measurement and the Hokupa'a results show that the infrared flux is dominated by the central point source.

3. Circumstellar Shocks

Optical spectroscopy (e.g. Guerrero & Manchado 1996) reveals emission lines from both the central V605 Aql nebula and the PNe A58 as well as a single Wolf-Rayet line ([C IV], FWHM $\sim 3000\,\mathrm{km\,s^{-1}}$) from the obscured final flash star. The PNe lines arise from both the front and back of the nebula and indicate an expansion velocity of $31\,\mathrm{km\,s^{-1}}$. Spectral lines of the central region are broad (FWHM $\sim 200\,\mathrm{km\,s^{-1}}$) and blue shifted, indicating an expansion velocity of $\sim 140\,\mathrm{km\,s^{-1}}$.

The wind off the central star has a velocity of several thousand $\mathrm{km\,s^{-1}}$. Since the central nebula spectral lines show an expansion velocity of $140\,\mathrm{km\,s^{-1}}$, we suggest that the interacting wind model of Kwok (1982) is appropriate to describe the V605 Aql circumstellar nebula. The collision of the fast wind with the remnant circumstellar shell results in an inner shock. This material is accel-

https://doi.org/10.1017/S025292110000138X Published online by Cambridge University Press

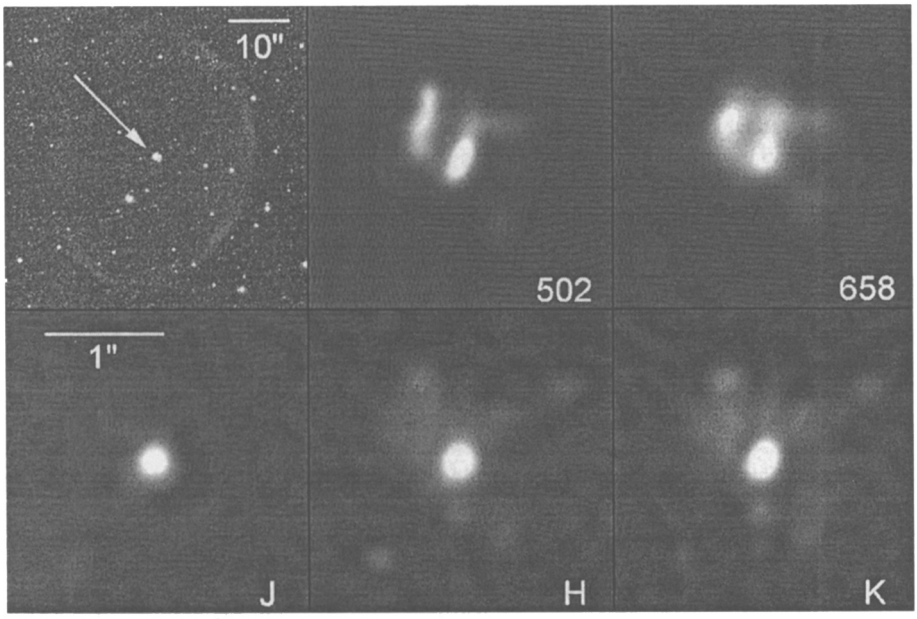

Figure 1. The top images are from HST/WFPC. The first image is larger scale and shows PNe A58 with V605 Aql marked by an arrow. The other two images show the inner 2″ in [O III] 5007 and [N II] 6584. Infrared images, J, H, and K', were obtained at the 8-m Gemini North telescope with the University of Hawaii Hokupa'a adaptive optics system. The FWHM of stars adjacent to V605 Aql was 0.17, 0.14, and 0.13 arcsec in the J, H, and K' filters, respectively.

https://doi.org/10.1017/S025292110000138X Published online by Cambridge University Press

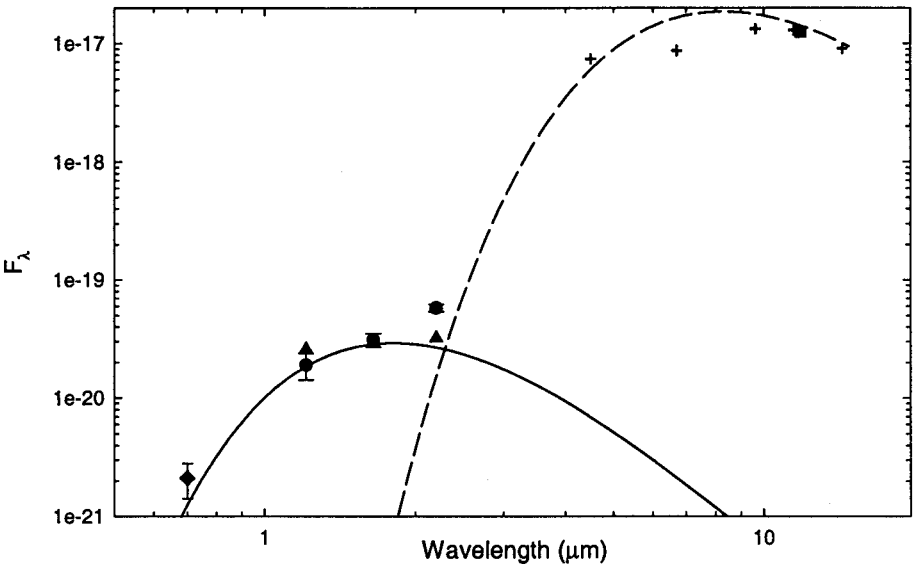

Figure 2. Spectral energy distribution of V605 Aql over the range 0.6 - 15 μm. Various values from the literature are compared to the current results (triangle - Hokupa'a; box - TIMMI2). The solid and dashed lines represent blackbody fits at 1600 K and 350 K, respectively.

erated and forms a shell which expands into the surrounding material creating a second shock zone.

4. Illumination of the Nebula

The 11.9 μm observation demonstrates that the star is surrounded by an optically thick region which reprocesses all the flux along the line of sight as thermal dust emission. In Fig. 2 we have fit two black bodies to the photometry. If we consider the observed K band flux as reprocessed energy radiating at the temperature (1600 K) which appears to fit the near infrared spectral energy distribution (Fig. 2), the spectral radiance at 2.2 μm of 3.9 $\mathrm{W\,cm^{-2}\,\mu m^{-1}\,sr^{-1}}$, coupled with the observed K = 14.6 ($5.6 \times 10^{-20}\,\mathrm{W\,cm^{-2}\,\mu m^{-1}}$) yields a radius of the emitting region of 1.4×10^{-5} arcsec. Material in grey body equilibrium at an apparent distance of 0.1 arcsec will then be at a temperature of $\sim$ 19 K. In the case that this model holds, the contribution of the thermal flux to the 2 μm image is negligible, raising the question of the source of the illumination of the infrared image. This puzzle has largely been solved by the used of a multiple grain size model which greatly enhances the thermal flux in the near infrared (Koller & Kimeswenger 2001).

The work of Koller & Kimeswenger (2001) also indicates that the black body fits shown in Fig. 2 are not correct representations of the temperature of the dust shell. A multiple grain size model has enhanced flux in the near-infrared while simultaneously fitting the mid-infrared flux. However, the disk

https://doi.org/10.1017/S025292110000138X Published online by Cambridge University Press

geometry requires a drop of temperature in an optically thick obscuring disk. A comprehensive model for the V605 Aql circumstellar nebula will include disk geometry with a realistic model of the grains and radiative transfer.

The optical lines are the result of shock excitation (Guerrero & Manchado 1996). The similarity of the optical and infrared images show that the dust and gas distributions are similar.

5. Shape of the Nebula

As noted above the V605 Aql circumstellar nebula appears bipolar. Four possible processes have been suggested for the formation of bipolar nebulae (Soker & Rappaport 2000). Three of these processes involve binary systems and appear not applicable to V605 Aql. The remaining process is the rapid rotation of a mass loosing single star (Reimers, Dorfi, & Höfner 2000). An interesting feature of V605 Aql is that the old, surrounding PNe A58 appears to be close to a spherical shell but does have a major axis aligned with the V605 Aql axis.

Several processes could be speculated to alter the geometry of the mass loss of the final flash star relative to the AGB star. One is the collision between the new fast wind and the previous slow wind. Another is enhanced rotation of the final flash star relative to the progenitor AGB star. Since the AGB star underwent extensive mass loss, conservation of angular momentum seems to require that the AGB stellar core not have been rotating at the same rate as the outer layers.

6. Conclusions

In both optical emission lines and near-infrared continuum (except perhaps J) V605 Aql has a resolved circumstellar nebula with a maximum diameter of ~ 1.6 arcsec. The nebula is asymmetric about the point source. The unresolved point source dominates the flux.

For a dust shell of 350 K and a 35000 K star, the outer shell to star radius ratio is 10^4. Similarly, the inner shell-to-star radius is ~ 400. Thus the geometry is compact and mass loss must be continuing vigorously, driven by continued helium burning. The distance to V605 Aql is ~ 3.8 kpc so the outer edge of the observed nebula is in agreement with the shell to star ratio.

The mass loss of V605 Aql has similarities to that of novae. In novae and final flash objects the onset of nuclear burning results in the development of a pseudo-photosphere 'fireball.' The expansion and cooling of the fireball then results in the formation of an optically thick dust shell. With a time scale that depends on the violence of the event and hence on the velocity of the ejecta, material can be seen expanding from the stellar remnant. However, unlike stellar cataclysmic explosions, final flash helium shell burning has an explosive onset followed by continued helium shell burning and continued mass loss. In the case of V605 Aql the shape of the mass loss from the AGB stage and final flash stage is quite different.

Acknowledgments. This paper is partly based on observations collected at the European Southern Observatory, Chile. NOAO is operated by the Asso-

ciation of Universities for Research in Astronomy, under cooperative agreement with the National Science Foundation. Thomas Lebzelter was supported by the Austrian Science Fund Project P14365-PHY. Josef Hron and K. Andre were supported by the Austrian Ministry for Education, Science and Culture. We would like to thank M. Sterzik (ESO) for his assistance with the TIMMI2 observations. Software created by Martin Sperl was essential in the reduction of the TIMMI2 observations. We would also like to thank Olivier Guyon, Dan Potter, and Francois Rigaut for their assistance with the Gemini North observations. This research made use of the SIMBAD database operated by CDS in Strasbourg, France and NASA's Astrophysics Data System Bibliographic Services.

References

Clayton, G. C., & De Marco, O. 1997, AJ, 114, 2679

Graves, J. E., Northcott, M. J., Roddier, F. J., Roddier, C. A., Potter, D., O'Connor, D. J., Rigaut, F. J., & Chun, M. R. 2000, Proc. SPIE, 4007, 26

Guerrero, M. A., & Manchado, A. 1996, ApJ, 472, 711

Hinkle, K., Joyce, R., Ridgway, S., Close, L., Lebzelter, T., Hron, J., & Andre, K. 2003, AJ, submitted.

Koller, J., & Kimeswenger, S. 2001, ApJ, 559, 419

Kwok, S. 1982, ApJ, 258, 280

Reimers, C., Dorfi, E. A., & Höfner, S. 2000, A&A, 354, 573

Soker, N., & Rappaport, S. 2000, ApJ, 538, 241